Available online at www.eccomasproceedia.org
Eccomas Proceedia COMPDYN (2021) 2808-2823

ECCOMAS
Proceedia

COMPDYN 2021
8th ECCOMAS Thematic Conference on
Computational Methods in Structural Dynamics and Earthquake Engineering
M. Papadrakakis, M. Fragiadakis (eds.)
Streamed from Athens, Greece, 28 - 30 June 2021

EXPERIMENTAL AND NUMERICAL INVESTIGATION OF THE PLASTIC CYCLIC BEHAVIOUR OF SIMPLE STEEL COUPONS

Alexandra Nalmpantidou, George C. Manos

Lab. of Strength of Materials and Structures
Dpt. Civil Engineering, A.U.Th.
Egnatia Odos, Panepistimioupoli
gcmanos@civil.auth.gr, a.nalmpantidou@posteo.de

Abstract

Steel beam-to-column connections under a cyclic sinusoidal loading history were studied. The investigation of the cyclic response of the steel beam-to-column connections contained an experimental and numerical part. The experimental part included a number of full-scale specimens having a cross section of IPE240 or IPE300 and a height of 1.0m which were rigidly connected to a much stiffer steel beam thus representing a steel beam-to-column connection. These specimens were tested to failure being subjected to a cyclic sinusoidal point load of continuously increasing amplitude. Next, a numerical study is performed in an effort to simulate the observed behaviour of these steel beam-to-column connections and their response is presented and discussed. The material test data for the numerical simulation of the steel beam-to-column connection were provided from simple steel coupons which were taken from the T-Beam specimens after testing. The cross-section of these coupons was 6.2mm x 8.0mm and their height equal to 16.5mm. A number of such simple steel coupons were tested having as main variable the nature of the load (monotonic or cyclic) and the variation of the loading frequency. From the observed behaviour it can be concluded that an increase in the strain rate results in an increase of the stress values beyond the yield. Next, a numerical study is performed in an effort to simulate the observed behaviour of these simple steel coupons. Experimental and numerical results of the material steel coupons are presented in this paper. It can be concluded that the combined constitutive law can be quite successful in yielding realistic prediction of the cyclic response provided the appropriate values for the parameters defining this constitutive law from the experimental test data, in combination with the option of the dynamic increase factor (DIF) in order to take into account the strain rate effect.

Keywords: Steel beam-to-column connection, Simple steel coupons, cyclic response, Numerical Simulation, Comparison of measured and predicted response, strain rate effects

ISSN:2623-3347 © 2021 The Authors. Published by Eccomas Proceedia.
Peer-review under responsibility of the organizing committee of COMPDYN 2021.
doi: 10.7712/120121.8676.19039

1 INTRODUCTION

Moment resistant frames are commonly used in seismic areas because of their excellence on seismic resistance whereby the performance of beam-to-column connections are of particular importance especially when these structures are subjected to strong earthquake ground motions ([1], [2], [3]). Usually these connections undergo large moment reversals during the earthquake excitation, thus it is important to exhibit stable plastic flexural response in order to provide dissipative capability, without the development of undesired damage patterns, and in this way prevent any kind of local or global instability.

In a previous investigation by Manos, Nalmpantidou and Anastasiadis ([10]) the performance of steel beam-to-column joints was studied first by examining steel beam-to-column welded joint specimens at the laboratory subjecting them to cyclic seismic-type low-cycle fatigue loading and then by numerically simulating the observed performance of the same specimens. Similar studies have been performed in the past by other researchers. Despite the fact that many similar experiments have been performed in the past ([4], [5]), this investigation provided at first hand all the information required for the numerical analyses. That is, the exact geometric and material characteristics of the specimens as well as specific information on the type of loading conditions and on the measured response. The numerical simulation was performed utilizing a commercial software package that is thought to be suitable to simulate the observed response and the non-linearity that developed and included large plastic strains and local instabilities.

One parameter that was found to be of significance in this investigation was the definition of the material characteristic of the steel T-Beam specimens that were investigated ([6], [8], [10], [11]). In order to assess the performance of structural steel components it is important to know the material properties. Quasi-static material tests are usually performed to obtain these parameters, however they may no longer represent the dynamic behaviour of the material during an earthquake, because as expected the loading frequency during an earthquake exceeds the loading frequency during the quasi-static material tests. In order to predict the response of a structure during an earthquake a good knowledge of the material behavior for the numerical simulation is important.

The T-Beam specimens were tested under cyclic load with the frequency of this loading being one of the variables that was studied. For this reason, it was necessary to study the material properties in light of the fact that the imposed cyclic loading was not of the constant slow-rate monotonic type that usually characterizes the material properties of steel structural elements. For this purpose, the following experimental sequence was carried out. From each of the tested steel T-Beams a number of coupon samples were taken, as is described in section 2. These samples were tested in axial tension/compression under cyclic loading with the frequency of the loading being one of the main variables. In addition, apart from these samples being tested by cyclic load additional samples of the same T-Beam specimens were tested applying the tension in a monotonic way. From all these tests results were obtained that shed some light on the influence of the nature of loading (cyclic or monotonic) as well as on the frequency of this loading. The results have been used to develop cyclic hardening parameters and dynamic increase factors suitable for incorporation into numerical models in order to predict the material behavior of structural members subjected to cyclic loading under several different frequencies. Summary results of this experimental sequence are presented and discussed in section 3. The numerical analysis of the observed performance is presented in section 4. The ABAQUS commercial software package was utilized for this purpose.

2 MATERIALS AND EXPERIMENTAL SETUP

The coupon samples for the tests aiming for the material characterization were obtained by removing parts of the flanges from the previously tested T-Beam specimens that were located away from the locations of the plastic hinge locations which developed during the T-Beam tests ([10],[12]). The testing of these T-Beam specimens is described in the work by Manos et al. ([10]) and is not repeated here.

Figure 1a. Coupon 6R1-6 (6.7mm x 6.7mm, ℓ =16mm)

Figure 1b. Coupon 6R1-5 (7.95mm x 7.80, ℓ =16mm)

The coupons to be tested were formed by machining the parts removed from the flanges, as shown in figures 1a and 1b. These coupons had a narrow central part of relatively small cross section with a small length (ℓ =16mm) and this part was designed to provide the necessary information for the material characterization. Through the two larger parts, which were provided with holes in order their attachment to the loading reaction frame to approximate pinned support conditions, the coupon was attached to the loading reaction frame. At the top and bottom of the coupon steel brackets are employed to attach the coupon sample using cylindrical pins. These brackets are in turn firmly attached to the reaction loading frame. At the top bracket a load cell is also attached that monitors the variation of the applied axial load.

The cross section of the narrow part remained constant all along its 16mm length. Its dimensions (x, y) were accurately measured (figures 2a, 2b and 2c). Moreover, strain gauges were attached at the middle of all the sides of this rectangular prismatic narrow part. These strain gauges were placed in the longitudinal direction of this steel prismatic part in order to measure the variation of the axial strain that developed during the variation of the axial load. The dimensions of the cross section of this narrow part combined with its length dictated almost uniform tension / compression conditions prohibiting the development of any distortions from local buckling, especially when large plastic strains developed in this narrow central part. Through the readings of the strain gauges the eccentricity of the axial load application could be checked and controlled.

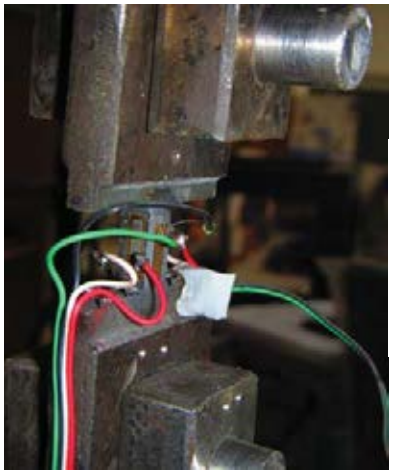

Figure 2a. Coupon 9R1-2 (6.2mm x 8.0mm, ℓ =16.5mm)

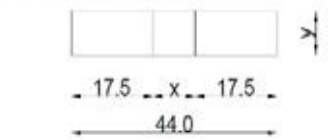

Figure 2b. Dimensions of the coupon

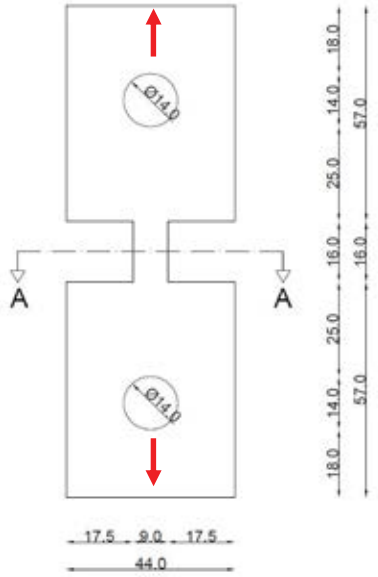

Figure 2c. Dimensions of the coupon

3 OBSERVED PERFORMANCE AND CORRESPONDING MEASUREMENTS.

As already mentioned, one of the main variables of this investigation was the nature of loading, being either cyclic or monotonic. The second variable was the frequency of the cyclic loading or the rate that the monotonic loading was applied, as will be indicated in what follows.

3.1 Monotonic loading

A summary of the results obtained when the specimens were subjected to monotonic axial tensile loading is presented below. The characterization of the applied load in terms of loading rate (slow or fast) and the origin code name of the T-Beam are mentioned in the presentation of these test results. In figure 3a the axial stress versus axial strain response is shown from two coupons taken from T-Beam 9R1; one of them was tested with slow strain rate whereas the other one with fast strain rate. As can be seen from this figure, this variation of the strain rate during the monotonic application of the applied load resulted in a significant change in the yield stress value as well as in the plasticized part of the response beyond the yield point. Next, figure 3b shows the response of axial stress versus axial strain from two coupons tested both at slow strain rate; one of them was taken from T-Beam 9R1 while the other from T-Beam 10R1. As can be seen from this figure, the response obtained from these two coupons is rather similar. By studying the two figures, we are led to the conclusion that increasing the strain rate from slow to fast leads to an increase in the yield stress as well as in the stress values beyond the yield point.

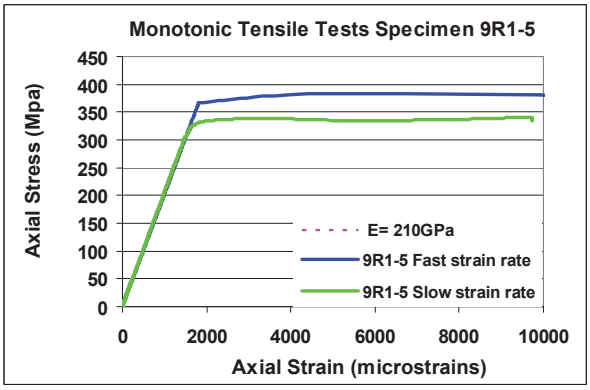

Figure 3a. Coupons taken from T-Beam 9R1 tested with slow and fast strain rate

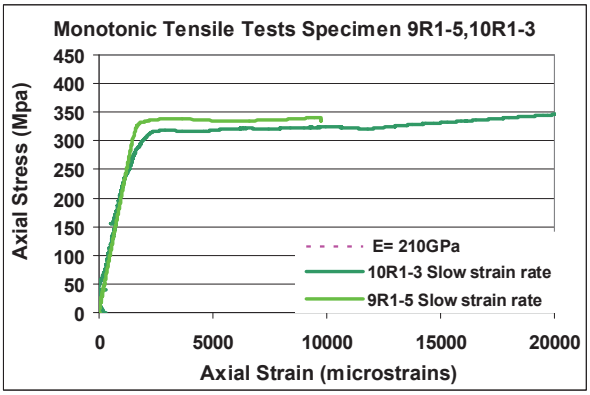

Figure3b. Coupons taken from T-Beam 9R1 and T-Beam 10R1 both tested with slow strain rate

3.2 Cyclic loading

Following on from our previous work ([12), this paper will present results from the material test coupons taken from the flanges of the T-Beam 8R1. In figure 4 and 5 the obtained axial stress versus axial strain responses are shown as they were measured and subjected to a number of cyclic loading tests. The strain rate during all these tests varied from fast to slow, as it resulted from the application of the axial tensile/compressive load from a sinusoidal variation with a frequency of 0.005Hz to 2.0Hz.

In figure 4a the cyclic response of a coupon taken from T-Beam 8R1 is shown. This response resulted by applying the axial load in a sinusoidal way with a frequency of 2.0Hz thus producing a rather fast strain rate. In figure 4b the cyclic response of a coupon also taken from T-Beam 8R1 is shown. This response resulted by applying the axial load in a sinusoidal way with a frequency of 0.005Hz thus producing a slow strain rate. Figure 5 shows the cyclic response of a coupon taken from T-Beam 8R1 obtained by applying the axial load in a sinusoidal way with a frequency ranging from 0.005Hz to 2.0Hz. The response obtained during the test whereby the cyclic load was varied with a frequency equal to 0.05Hz is considered as a rather slow strain rate test whereas the one with a frequency equal to 0.1Hz as a rather moderately fast strain rate test. Finally, the response obtained during the test whereby the cyclic load was varied with a frequency equal to 2.0Hz is considered as a rather fast strain rate test.

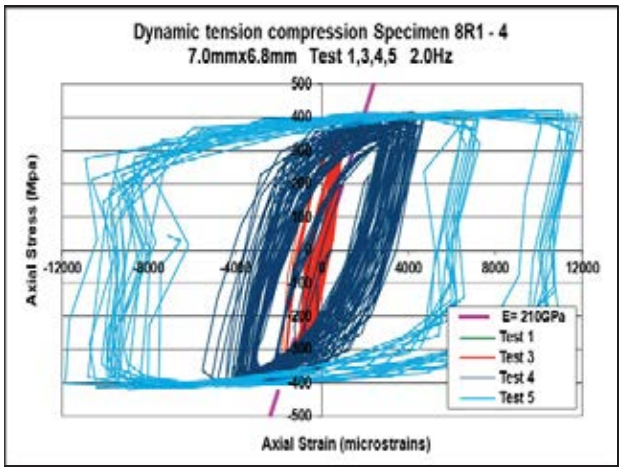

Figure 4a. Cyclic response with axial load varying in a sinusoidal way with a frequency of 2.0Hz. Coupon taken from T-Beam 8R1 tested with a rather fast strain rate

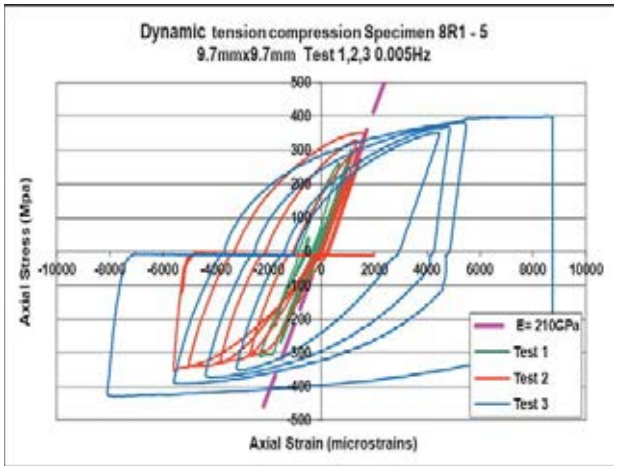

Figure 4b. Cyclic response with axial load varying in a sinusoidal way with a frequency of 0.005Hz. Coupon taken from T-Beam 8R1 tested with a slow strain rate

As can be seen from these figures (4a, 4b, and 5) the yield point can be hardly distinguished from the obtained axial stress versus axial strain response. However, as can be seen in figure 5, the variation of the strain rate during the cyclic application of the applied load resulted in a significant change in the plasticized part of the response beyond yield as it was also observed in figure 3a for the monotonic application of the load. It can be concluded from both figures 3a and 5 that the increase in the strain rate results in a noticeable increase both at the yield stress as well as at the stress values beyond the yield point for strain values larger that the yield strain.

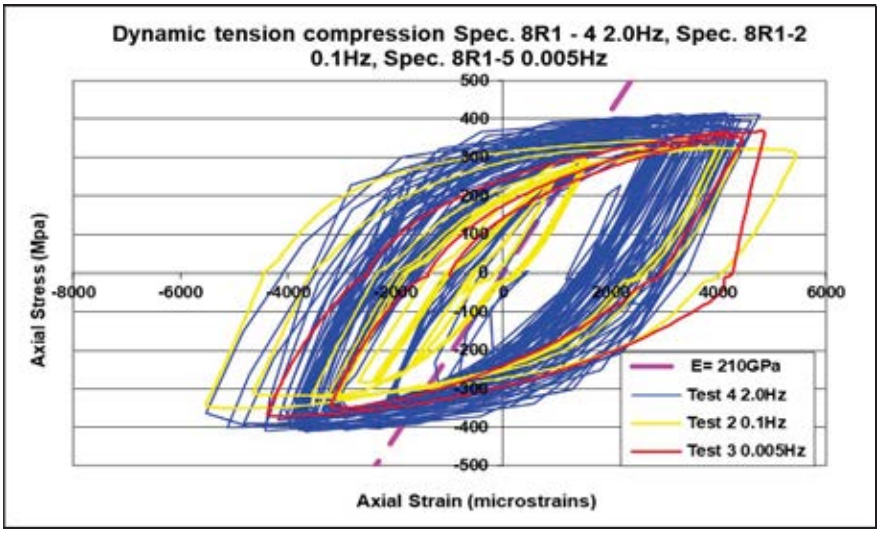

Figure 5. Cyclic response when axial load is varying in a sinusoidal way with frequency values in the range from 0.005Hz to 2.0Hz. Coupons taken from T-Beam 8R1 tested with slow as well as with fast strain rate

In figure 6, a comparison between the axial stress versus axial strain response from four coupons under cyclic and monotonic loading is shown; one of them is taken from T-Beam 8R1, one of them is taken from T-Beam 10R1 and two of them are taken from T-Beam 9R1. Coupon 8R1 was tested with a cyclic loading frequency equal to 2.0Hz (Tests 3, 4, 5) producing a rather fast strain rate. Two coupons from T-Beam 9R1 were tested by applying the tensile

load in a monotonic way; one of them with a slow strain rate (INSTRON static 9R1-5) and the other one with a fast strain rate (INSTRON quick 9R1-5). Finally, the fourth specimen was taken from T-Beam 10R1 and was tested by applying monotonic load with a slow strain rate (INSTRON static 10R1-3). The two main observations that were made before can also be seen in this figure.

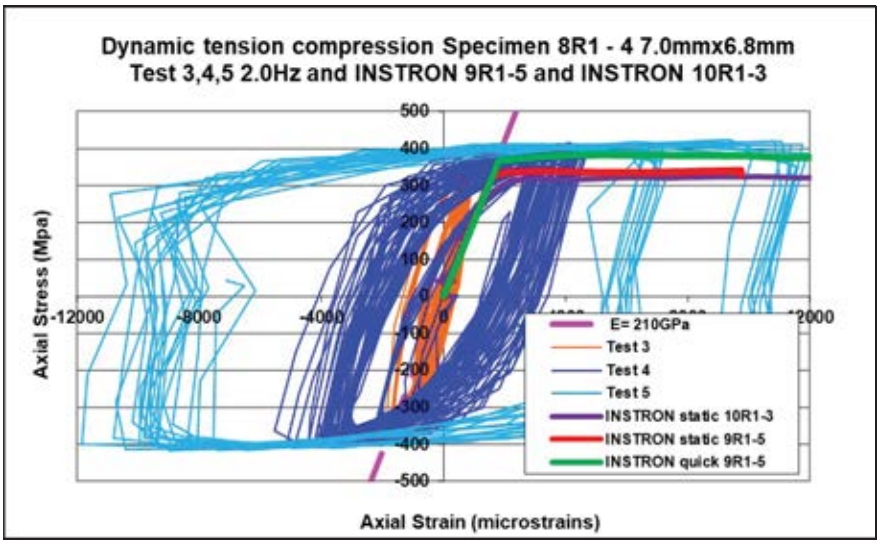

Figure 6. Monotonic / cyclic axial stress - strain response. The cyclic axial load is varying in a sinusoidal way with frequency value equal to 2.0Hz (T-Beam 8R1). Monotonic response from coupons taken from T-Beam 9R1 and 10R1 tested either with slow or with fast strain rate

From the above observed performance it can again be concluded that,

a) During the monotonic application of the load an increase in the strain rate resulted in an increase in the yield stress value as well as in the stress values of the plasticized part of the response beyond the yield point. In addition to this the observed axial stress versus axial strain response from different coupons subjected to the same slow strain rate monotonic load is quite similar.

b) The application of the cyclic load with slow, moderately fast or rather fast strain rate resulted in axial stress versus axial strain response whereby the yield point is hardly distinguishable but despite of this the strain rate effect can be clearly seen. Furthermore the application of the cyclic load with slow, moderately fast or rather fast strain rate resulted in axial stress versus axial strain response that has stress values beyond the yield point that exhibit a noticeable increase with the increase in the strain rate.

c) From the limited results presented here the effect of the cyclic nature of the loading results in a more pronounced increase of the stress values with the increase in the strain rate than when the load is applied in a monotonic way.

4 NUMERICAL SIMULATION OF THE TENSION AND CYCLIC TESTS

4.1 Numerical modeling.

As mentioned in section 2 simple specimens having the shape of an orthogonal prism were taken from the flanges and were applied to monotonic tension or / and to cyclic tensile / compressive load with a sinusoidal time variation having a given amplitude and frequency. A

number of such simple specimens were tested and their results are presented and discussed in section 3 having as main variable the variation of the loading frequency and the nature of the loading (monotonic or cyclic). In order to simulate numerically the behavior of these specimens a numerical study was performed utilizing the commercial software package ABAQUS [7].

The orthogonal prism of the experimental sequence (figure 7a), which was represented through the finite element 2-D mesh, is shown in figures 7b. The prism was considered to be represented with absolute fixity conditions in the numerical simulation on the top side whereas on the bottom side either the monotonic or the cyclic load was applied. The other two sides were left unconstrained. However, the rigid body in-plane as well as the out-of-plane horizontal displacement response was also constrained.

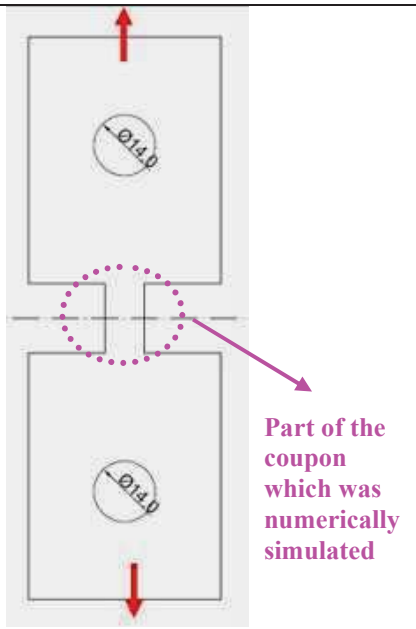

Figure 7a. The tested coupon and the orthogonal steel prism which was numerically simulated, as shown in figure 7b (see also figures 2a, 2b and 2c)

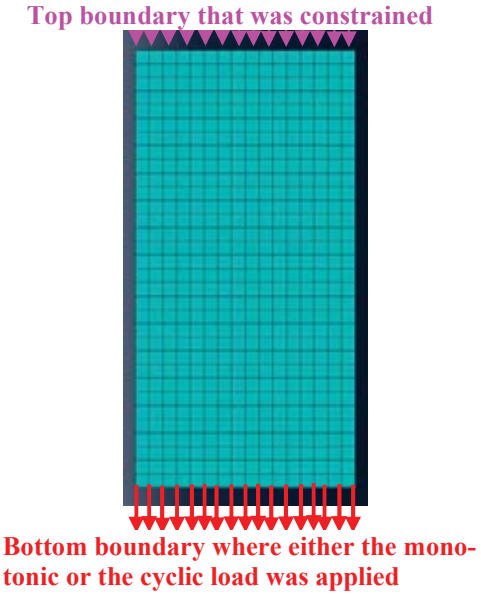

Figure 7b. The ABAQUS numerical simulation of the orthogonal steel prism of the tested coupon (see figure 7a and figures 2a, 2b and 2c)

In order to simulate the variation of the load in time as either fast or slow monotonic load or as cyclic load with varying sinusoidal cyclic frequency, the displacement control option was utilized whereby an imposed displacement was defined as a function of time and displacement amplitude. Dynamic implicit analyses were in-order for this software to take into account the different load frequencies. Following the load variation that was applied during testing the numerical analyses were also performed with monotonic load (with either slow or fast strain rate) and with cyclic load (again with either slow, moderate or fast strain rate). The imposed displacement variation was introduced to the software in tabular form identical with the one that was applied to the corresponding specimen during the experimental sequence. The adopted discretization scheme (figure 7b) is believed to be considerably fine in an effort to capture numerically the observed behavior.

4.2 Material modeling

In the framework of the numerical investigation a parametric study was conducted that focused on the way the steel material properties were introduced in the numerical simulation. In our previous work two different approaches were tried ([12]). According to the first approach

the measured tensile steel properties were modified accordingly in order to be introduced in the numerical simulation through the ABAQUS combined hardening material constitutive law whereas in the second approach the measured properties were introduced in the numerical simulation through the ABAQUS isotropic hardening constitutive law. Furthermore in both cases different yield stress ratios for different strain rates were taken into account.

In this work the focus lies in the numerical simulation of the material tests through the ABAQUS combined hardening material constitutive law. There are several ways in this commercial software package [7] to define a combined hardening material constitutive law in order to capture the cyclic response of a specimen. The evolution law of this model consists of two components: a nonlinear kinematic hardening component, which describes the translation of the yield surface in stress space through the back-stress, and an isotropic hardening component, which describes the change of the equivalent stress defining the size of the yield surface, as a function of plastic deformation [7]. In the present study the combined hardening constitutive law is defined through the values that are given to certain relevant parameters. For the nonlinear kinematic hardening component these parameters are a) $\sigma|_0$, the yield stress at zero equivalent plastic strain, b) C_k and γ_k (material constants that can be calibrated from test data) and for the isotropic hardening model these parameters are c) $\sigma|_0$, equivalent yield stress, d) Q_∞ and b_{iso} (material constants that can be calibrated from test data). Values for these parameters were calculated from the test data that were obtained from the experimental process from the tests of steel samples and were utilized in the parametric study that was performed in the present work. The nonlinear kinematic hardening component of the model defines the change of back-stress α and is given by Equation (1). All stress strain data are taken from a stabilized cycle from the test data as shown in figure 8.

$$\alpha_k = C_k / \gamma_k \, (1 - e^{-\gamma_k \, \varepsilon pl}) + \alpha_{k,1} \, e^{-\gamma k \, \varepsilon pl} \tag{1}$$

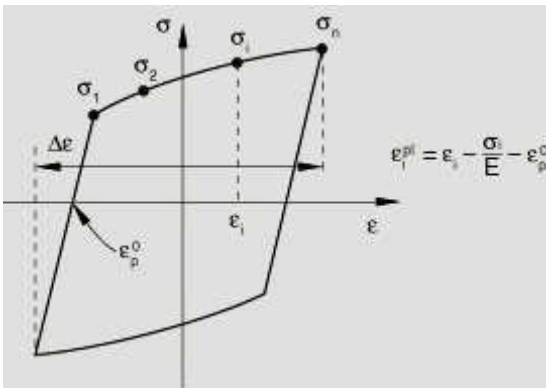

Figure 8. Stress strain data for a stabilized cycle

The isotropic component defines the change of the size of the yield surface σ^0 as a function of equivalent plastic strain ε^p as shown in figure 9 and is given by Equation (2).

$$\sigma^0 = \sigma|_0 + Q_\infty \, (1 - e^{biso \, \varepsilon p}) \tag{2}$$

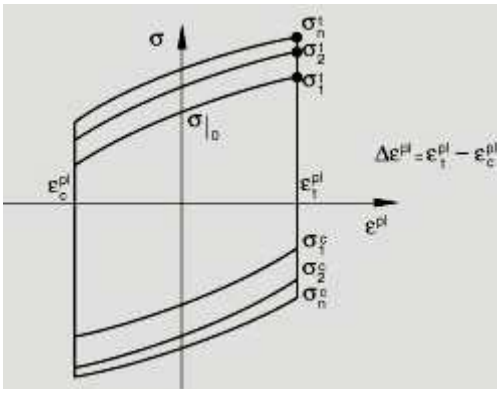

Figure 9. Symmetric strain cycle

Abaqus allows the specification of strain rates effects with the option of rate dependent data at combined and isotropic hardening constitutive law. In order to define the strain rate effect the use of a dynamic increase factor (DIF) was utilized based on the work of Malvar and Crawford [9]. The same values for DIF that were calculate and introduced as input in tabular form in terms of a ratio of the yield stress versus the equivalent plastic strain rate to be used in the particular case being analyzed, from our previous work [12] are also being used in this paper. The work of Malvar and Crawford [9] is based on numerous experimental data from a literature review on the effects of strain rates on the properties of steel reinforcing bars for reinforced concrete structural elements. The dynamic increase factor (DIF) is the amplification by DIF of the value a certain mechanical property (yield stress or maximum stress) has under low strain rate loading conditions (static) to another condition whereby because of the nature of loading (dynamic) the strain rate has a larger value than before. A relationship is proposed by Malvar and Crawford ([9]) that a DIF value can be derived for a given strain rate increase and thus evaluate through this DIF the corresponding for this increased strain rate amplified yield and ultimate stress values. This formulation is valid for bars with yield stresses between 290 and 710 MPa and for strain rates between 10^{-4} sec^{-1} and 225 sec^{-1}. Figure 10 depicts the variation of DIF with the variation of the strain rate. This approach was presently followed use as reference control properties the yield stress found for the slow rate monotonic axial tension test with coupon 9R1-5 (see figure 5).

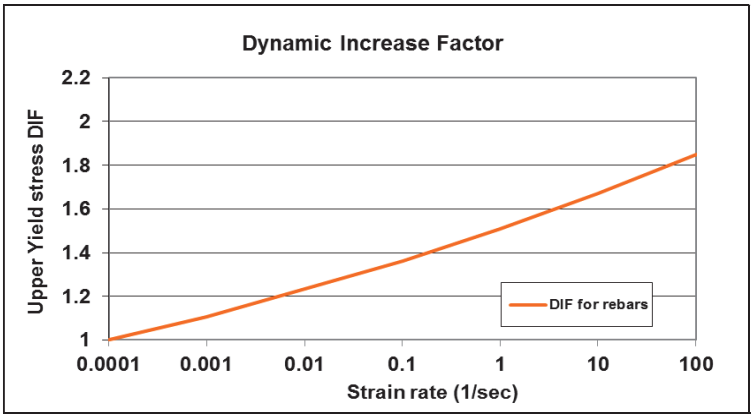

Figure 10. Dynamic increase factor which has been considered for the numerical investigation

4.3 Numerical results for monotonic axial tensile load cases

Figure 11 shows a comparison between the axial stress – axial strain monotonic tensile response obtained from the numerical analysis of coupon 9R1-5 and 10-3 loaded under slow strain rate conditions (duration of loading 700 seconds) and coupon 9R1-5 loaded under fast strain rate conditions (duration of loading 2.5 seconds) for both constitutive laws of isotropic hardening and combined hardening together with the option of the DIF.

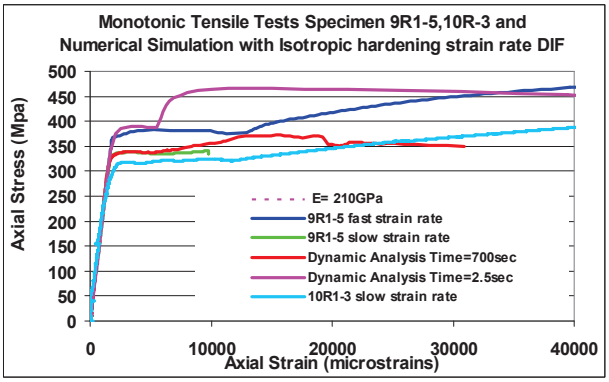

Figure 11a. Monotonic axial tension numerical simulation with isotropic hardening constitutive law for coupon 9R1-5 and 10R-3 for strain values up to 40000 microstrains.

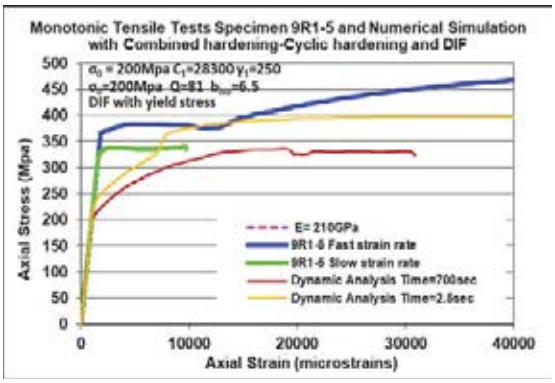

Figure 11b. Monotonic axial tension numerical simulation with combined hardening constitutive law for coupon 9R1-5 for strain values up to 40000 microstrains.

As can be seen in figure 11a, the numerical simulation including the isotropic hardening with the DIF option is quite sensitive to the effect of the strain rate variation. Moreover, the numerical response agrees quite well with the observed response for strain values smaller than 6000 micro-strains. In the case of the slow strain rate there is a certain discrepancy between predicted and observed stress values for strains larger than 10000 micro-strains and smaller than 20000 micro-strains. Similarly, in the case of the fast strain rate there is again a certain discrepancy between predicted and observed stress values for strains larger than 6000 micro-strains and smaller than 25000 micro-strains.

In figure 11b depicts the axial stress-strain numerical response employing combined hardening constitutive low together with the DIF options for coupons 9R1-5 submitted to monotonic tension load with slow strain rate conditions (duration of loading 700 seconds) and with fast strain rate conditions (duration of loading 2.5sec). The material parameters that were calculated from test data from test coupons that were taken from T-Beam 9R1 and were used to define the combined hardening constitutive law with cycling hardening are:

Combined hardening parameters:
Yield stress at plastic strain $\sigma|_0$=200Mpa,
Kinematic Hardening Parameter C_k=28300
Gamma γ_k=250
Cyclic hardening paraneters:
Equivalent stress $\sigma|_0$=200Mpa
Q-Infinity parameter Q_∞=81
Hardening parameter b_{iso}=6.5

As indicated in figure 11b there is no good agreement between numerical simulation and measured response. The reason for that could be that the kinematic hardening model, which includes the combined hardening, is for simulating the cyclic loading of metals and not monotonic tensile behaviour (Abaqus). From the relevant graph it can be easily seen that a value for the yield point equal to 200Mpa is assigned for the slow strain rate tension test (duration of loading 700 sec) which is the same value of the yield stress at zero equivalent plastic strain from a stabilised cycle $\sigma|_0$=200Mpa. This value was obtained from the test data of the cycling loading. Furthermore, the numerical simulation is quite sensitive to the effect of the strain rate variation, as can be seen in the plotted response. An increase of the yield and ultimate stress can be seen from the case when the specimen is subjected to a relatively slow loading (which corresponds to a slow strain rate) to the case when the specimen is subjected to a relatively fast loading (which corresponds to a fast strain rate).

4.4 Numerical results for cyclic axial tension / compression load cases

This section presents numerical results of the experimental investigation carried out with material test coupons obtained from T-Beam 8 under cyclic axial tension /compression load cases. The necessary material parameters for the numerical simulation were calculated from the experimental data based on Equations (1) and (2) mentioned in section 4.2. These values are as follows:

Combined hardening parameters:
Yield stress at plastic strain $\sigma|_0$=200-220Mpa,
Kinematic Hardening Parameter C_k=34000
Gamma γ_k=250
Cyclic hardening paraneters:
Equivalent stress $\sigma|_0$=200-220Mpa
Q-Infinity parameter Q_∞=85
Hardening parameter b_{iso}=6.5

Figures 12a and 12b depict the axial stress-strain numerical response employing combined hardening constitutive law with cyclic hardening together with the DIF options for coupons 8R1-5 and 8R1-3 submitted to cyclic tension / compression load resulting in a slow strain rate condition (variation in time of the sinusoidal cyclic load equal to 0.005Hz) and in a moderately slow strain rate condition (variation in time of the sinusoidal cyclic load equal to 0.01Hz). As indicated in these figures a reasonably good agreement between numerical predictions and measured response was achieved for values of the parameters $\sigma|_0$=220Mpa, C_k=34000, γ_k=250, Q_∞=85, b_{iso}=6.5 for a cyclic load equal to 0.005Hz and a cyclic load equal to 0.01Hz. This good agreement between measured and predicted values can be seen for the yield and ultimate stress values as well as for the shape of the hysteretic loops.

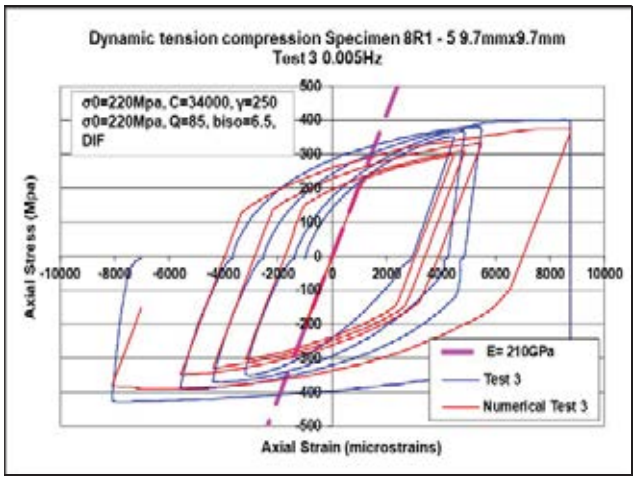

Figure 12a. Numerical axial stress strain response employing combined hardening constitutive law for coupons 8R1-5 submitted to cyclic tension/compression load resulting in a slow strain rate

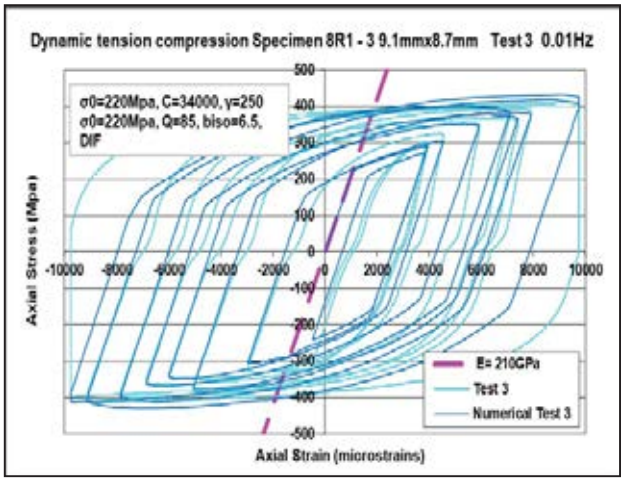

Figure 12b. Numerical axial stress strain response employing combined hardening constitutive law for coupons 8R1-3 submitted to cyclic tension/compression load resulting in a moderately slow strain rate

Figures 13a and 13b depict the axial stress-strain numerical response employing combined hardening constitutive law with cyclic hardening together with the DIF options for coupons 8R1-2 and 8R1-4 submitted to cyclic tension / compression load resulting in a moderately fast strain rate condition (variation in time of the sinusoidal cyclic load equal to 0.1Hz) and in a fast strain rate condition (variation in time of the sinusoidal cyclic load equal to 2.0Hz). As indicated in these figures, reasonably good agreement between numerical predictions and measured response was achieved adopting values of the parameters $\sigma|_0$=200Mpa, C_k=34000, γ_k=250, Q_∞=85, b_{iso}=6.5 for cyclic loads applied with frequencies equal to either 0.1Hz or 2.0Hz. For numerically simulating these relatively high loading frequency tests the value of $\sigma|_0$ equal to 200Mpa was adopted the yield stress at plastic strain and the equivalent stress instead of 220Mpa, which was used in the numerical simulation for the relatively load loading frequencies of 0.005Hz and 0.01Hz. This value of 200Mpa led to a better agreement between the experimental results and the numerical simulation for the yield and ultimate stress values as well as for the shape of the hysteretic loops.

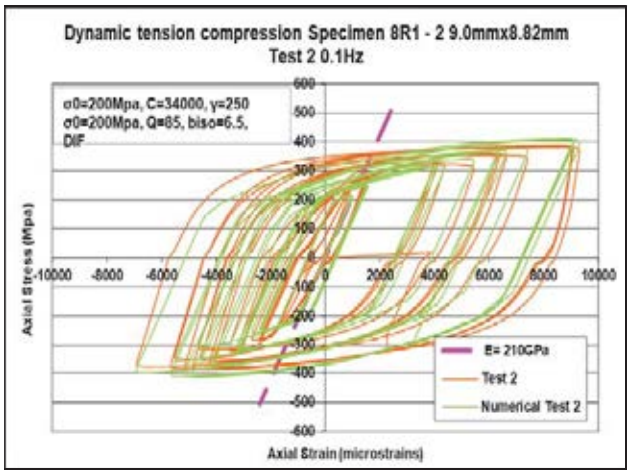

Figure 13a. Numerical axial stress strain response employing combined hardening constitutive law for coupons 8R1-5 submitted to cyclic tension/compression load resulting in a slow strain rate

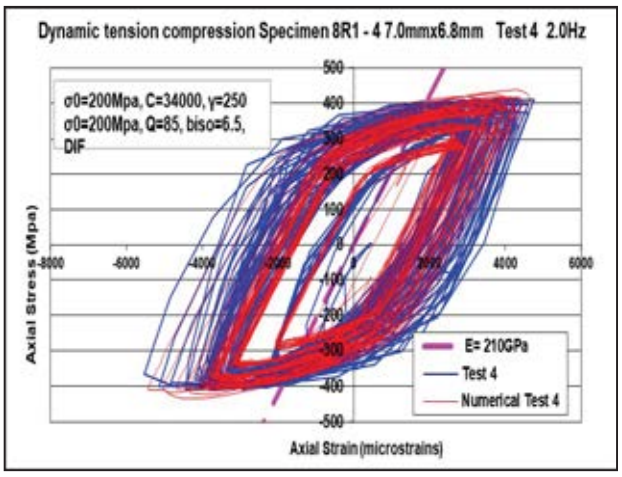

Figure 13b. Numerical axial stress strain response employing combined hardening constitutive law for coupons 8R1-3 submitted to cyclic tension/compression load resulting in a moderately slow strain rate

From this numerical study it can again be concluded that a numerical simulation based on the combined constitutive law employing values of the necessary parameters from test data (such as $\sigma|_0$, the yield stress at zero equivalent plastic strain, and C_k and γ_k the material constants) is quite successful in yielding realistic predictions of the cyclic response. Moreover, utilising the an inclusion of the DIF option, such a numerical simulation can be also sensitive to the observed strain rate effect. Therefore, it is reasonable to believe that it would also be successful in simulating the behaviour of more complex structural elements under a variety of loading which can result in different strain rate conditions.

5 CONCLUSIONS

- An extensive experimental sequence was conducted testing relatively small dimension coupons to axial monotonic or cyclic loading with a variety of strain rate conditions. These coupons were formed from steel parts taken from the flanges of T-beam steel section that were previously tested to destruction by cyclic seismic-type loading. The current study is an extension of the previous research in an effort to first quantify the strain rate effect in a controlled way and next to be able to effectively simulated utilizing existing numerical tools. From the current investigation the following findings could be stated.
- An increase in the strain rate during the monotonic application of the load resulted in an increase in the yield stress value as well as in the stress values of the plasticized part of the response beyond the yield point.
- Additional experimental data from the analysis of more T-Beams under cyclic loading to be added to the existing ones led to the same conclusion as before that
  a)The application of the cyclic load with slow, moderately fast or rather fast strain rate resulted in axial stress versus axial strain response whereby the yield point is hardly distinguishable. Thus the strain rate effect can be clearly seen.
  b)The application of the cyclic load with slow, moderately fast or rather fast strain rate resulted in axial stress versus axial strain response that has stress values beyond the yield point that exhibit a noticeable increase with the increase in the strain rate.

- From the subsequent numerical study it can be concluded that the combined constitutive law is quite successful in yielding realistic prediction of the cyclic response but not of the monotonic tensile response; the appropriate values of the parameters defining this constitutive law (such as $\sigma|_0$, the yield stress at zero equivalent plastic strain, C_k, γ_k, Q_∞ and b_{iso} the material constants) must be calibrated from test data. In this case, the numerical simulation employing the same material constitutive law together with an DIF inclusion is reasonable to believe that it would also be successful in simulating the behaviour of more complex structural elements for loading introducing a variety of strain rate conditions.
- Both the experimental and the numerical part of this study are still under way; thus the above conclusions should be considered as preliminary.

ACKNOWLEDGEMENTS

The authors would like to acknowledge the assistance of M. Theofanous, Dr. Civil Engineer, Lecturer at the Department of Civil Engineering of the University of Birmingham, for all his valuable advice related to the numerical simulation. The technical assistance of T. Koukouftopoulos in preparing the experimental arrangement is also gratefully acknowledged.

- To the memory of Hiroshi Akiyama, Professor of the University of Tokyo, Japan and of Heki Shibata, Professor of Industrial Science, University of Tokyo, Japan.

REFERENCES

[1] Akiyama H. Earthquake-Resistant Limit-State Design for Buildings. University of Tokyo Press: Tokyo, 1985.

[2] Anastasiadis A., Mosoarca M., Gioncu V., Mazzolani F. M., "Some thoughts for the prediction of the local inelastic capacity of MRF subjected to seismic actions", 8th STESSA Conf. on the Behavior of Steel Structures in Seismic Areas, Tongji Univ., Songhai China, July 2015.

[3] Ballio Giulio &. Castiglioni, Carlo A, "Seismic Behaviour of Steel Sections", J. Construct. Steel Research 29 (1994) 21-54

[4] Castiglioni Carlo A., Mouzakis Harris P., Carydis Panayotis Gr. (2007): "Constant and Variable Amplitude Cyclic Behavior of Welded Steel Beam-to-Column Connections", Journal of Earthquake Engineering, 11:876–902, 2007, 11:6, 876-902, doi.org/10.1080/13632460601188027.

[5] El Hassouni A, Plumier A., Cherrabi A. "Experimental and numerical analysis of the strain-rate effect on fully welded connections", Journal of Constructional Steel Research (2010), doi 10.1016/j.jcsr.2010.09.02

[6] Gioncu V, Petcu D. "Available rotation capacity of wide-flange beam and beam-columns part 1, 2.", Journal of Constructional Steel Research 1997; 43: 161-244.

[7] Hibbitt, Karlsson, Sorensen. Inc. ABAQUS user's manual volumes I–V and ABAQUS CAE manual. Version 6.10.1. Pawtucket, USA; 2010.

[8] Lee Kyungkoo and Stojadinovic Bozidar, "Low-cycle fatigue limit on seismic rotation capacity for US steel moment connections", 13th World Conference on Earthquake Engineering, Vancouver, B.C., Canada, August 1-6, 2004, Paper No. 90.

[9] Malvar, L. J. and John E. Crawford J. E. (1998), "Dynamic increase factor for steel reinforcing bars", Twenty-Eighth DDESB Seminar, Orlando, FL.

[10] Manos G.C., A. Nalmpantidou A., Kourtides A., Anastasiadis A., (2015), "Cyclic response of a steel beam to column conection – an experimental and numerical study", CompDyn 2015, M. Papadrakakis, V. Papadopoulos, V. Plevris (eds.), Crete Island, Greece, 25–27 May 2015.

[11] Vayas I. "Investigation of the cyclic behavior of steel beams by application of low-cycle fatigue criteria." Behavior of Steel Structures in Seismic Areas STESSA 1997; 350-357.

[12] Manos G.C., A. Nalmpantidou A., (2019), "Experimental and numerical study of the cyclic behaviour of a steel beam-to-column connection", CompDyn 2019, M. Papadrakakis, M.Fragiadakis (eds.), Crete Island, Greece, 24–26 June 2019.